Magnetohydrodynamic convection of Cu-water nanofluid in a square cavity with a circular cylinder

Canan Bozkaya

Abstract—The hydromagnetic free convection of a Cu-water nanofluid in a square cavity involving an adiabatic circular cylinder is numerically investigated in the presence of an inclined uniform magnetic field. The left and right walls of the cavity are kept at constant hot and cold temperatures, respectively, while the horizontal walls are assumed to be adiabatic. The coupled nonlinear equations of mass, momentum and energy governing the present problem are discretized using the dual reciprocity boundary element method which is a boundary only nature technique treating the nonlinear terms by the use of radial basis functions. The flow and thermal fields are analyzed through streamline, isotherm, and average Nusselt number plots for a wide range of controlling parameters, such as Rayleigh and Hartmann numbers, the nanoparticle volume fraction and the inclination angle of the magnetic field. The results reveal that heat transfer and fluid flow are strongly affected by the presence of the circular cylinder and the inclined magnetic field.

Keywords—MHD, natural convection, nanofluids, DRBEM.

I. Introduction

CONVECTION flow and heat transfer in enclosures have been investigated by many researchers due to their importance in many engineering applications such as nuclear reactors, design of solar collectors, thermal design of buildings, lakes and reservoirs, air conditioning and cooling of electronic devices, food processing, crystal growth and coating solidification. The fluids with small sized nanoparticles suspended in them are called nanofluids. Due to small sizes and large specific surface areas of the nanoparticles, nanofluids have superior properties like long-term stability, homogeneity and especially high thermal conductivity when compared to conventional base fluids such as water and ethylene glycol. Thus, recently nanofluids have been extensively analyzed in the heat transfer applications due to their potential in the enhancement of heat transfer with minimum pressure drop. When the fluid is electrically conducting and the fluid flow is due to convection under the influence of a magnetic field, the fluid experiences a Lorentz force. This force affects the heat transfer rate and reduces the velocity of the fluid particles which is the well-known retarding effect of magnetic field on the convective flow. The free convection is under the effect of a magnetic field in many applications such as fusion reactor, thermal insulation systems, crystal growth and metal casting. Therefore, considering a combined effect of magnetic field and addition of nanoparticles becomes crucial in the study of convection flow of an electrically conducting fluid to control the heat transfer and fluid flow characteristics.

C. Bozkaya is with the Department of Mathematics, Middle East Technical University, 06800, Ankara, Turkey e-mail: bcanan@metu.edu.tr

There are many works on the numerical solution of the natural convection in a nanofluid filled cavity under the influence of an externally applied magnetic field with different thermal boundary conditions. Ghasemi et al. [1] and Teamah et al. [2] have investigated the effect of the horizontal magnetic field on heat transfer in a square enclosure by using control volume (CV) based on Patankar's SIMPLE algorithm. A numerical solution to magnetohydrodynamic (MHD) natural convection flow in a square cavity by using Lattice Boltzmann method (LBM) has been analyzed in the works [3], [4] under different thermal wall conditions. They found that heat transfer enhancement with the growth of solid volume fraction depends on Hartmann and Rayleigh numbers. Rahman et al. [5] have studied Buongiorno's model for hydrodynamic free convection flow in a triangular cavity filled with nanofluid by Galerkin weighted residual finite element method (FEM). The results showed that the heat transfer rate can be decreased with increasing Hartmann number but it can be increased by increasing Rayleigh number and by reducing the diameter of the nanoparticles. Tezer-Sezgin et al. [6] have solved the natural convection nanofluid flow in a square enclosure in presence of an inclined magnetic field using both FEM and dual reciprocity boundary element methods (DRBEM). The hydromagnetic nanofluid natural convection flow has been further solved numerically in different geometries. Ghasemi [7] have studied the natural convection in an U-shaped enclosure filled with nanofluid with the use of control volume formulation with SIMPLE algorithm. They observed that the heat transfer rate increases as Rayleigh number increases while it decreases for higher values of Hartmann number. The natural convection in an inclined L-shaped nanofluid filled cavity in the presence of inclined magnetic field has been solved by the finite difference method (FDM) in the work of Elshehabey [8], and their results revealed that a good enhancement in the heat transfer rate is obtained by adding cooper nanoparticles to the base fluid. Bondareva et al. [9] have also used FDM for the solution of MHD natural convection in an inclined wavy porous cavity filled with a nanofluid to investigate the effects of Hartmann number, inclination angles of the cavity on the heat transfer and fluid flow. Sheikholeslami et al. [10] have investigated the heat transfer characteristics of unsteady nanofluid flow between parallel plates by using differential transformation method. It is found that Nusselt number increase with Hartmann, Eckert and Schmidt numbers but it decreases with augment of squeeze number.

In this study our focus is on the MHD natural convection flow in nanofluid filled enclosures with a detached body placed inside it. The thermal boundary conditions, the shape, location

and size of the body is of great interest in heat transfer applications. In fact, the presence of a solid body has a direct effect on the fluid flow and hence on the heat transfer. There have been studies considering the combined effect of the magnetic field and internal solid bodies on the nanofluid natural convection flow in cavities by using domain decomposition techniques such as FEM, FVM and LBM. Aminossadati [11] have analyzed the cooling of a right triangular heat source in a triangular cavity under the influence of a horizontal magnetic field using CV formulation. The heat transfer enhancement of nanofluid filled square cavity with a circular disk have been investigated by Kobra et al. [12] with FEM. Selimefendigil and Özturk [13] have worked on the impact of different shaped obstacles on the natural convection and entropy generation of nanofluid filled cavity with inclined magnetic field. They employed Galerkin weighted residual FEM for the discretization of the equations and it was found that the square shaped bodies deteriorates the averaged heat transfer more than the circular and diamond shape bodies compared to the case without obstacle at high Rayleigh number 10^6. Zhang and Che [14] has developed a two-dimensional double multiple-relaxation-time thermal LBM to simulate the MHD flow and heat transfer of Cu-water nanofluids in an inclined cavity with four heat sources placed inside the cavity. Their results showed that the average Nusselt number increases significantly with the increase of nanoparticles volume fraction, but it decreases in the presence of magnetic field at any Rayleigh number and inclination angles.

We aim here to analyze numerically the natural convection flow and the heat transfer in a closed square cavity filled with Cu-water nanofluid which involves an adiabatic circular cylinder under the effect of an externally applied inclined magnetic field. To the best of authors knowledge and based on the above literature survey, no work has been reported on the dual reciprocity BEM solution, which reduces the dimension of the problem by discretizing only the boundary of the problem, to the specified MHD natural convection problem which may be encountered in the area of coating, food processing, cooling systems, nuclear and solar reactors and many more. The present study focuses on incorporating this issue with the effect of controlling parameters including Rayleigh and Hartmann numbers, nanoparticle volume fraction and the inclination angle of the magnetic field. The heat transfer enhancement is also analyzed through average Nusselt number at various combination of aforementioned controlling parameters along the hot left wall of the cavity both in the presence and absence of the inner circular cylinder.

II. Mathematical formulation

The schematic view of the problem of a two-dimensional square cavity of height ℓ with a circular cylinder of diameter d placed at the center of the cavity is illustrated in Figure 1. The left and right walls are maintained at isothermal hot T_h and cold T_c temperatures, respectively. On the horizontal walls and on the cylinder surface adiabatic boundary condition is assumed. A uniform inclined magnetic field of strength B_0 is applied forming an angle γ with the x-axis and the

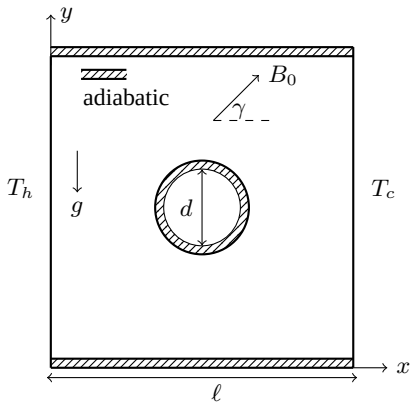

Fig. 1. Geometry of the physical problem with boundary conditions.

gravity acts in the negative y-direction. The cavity is filled with a Newtonian Cu-water nanofluid, and the flow generated inside the cavity is assumed to be steady, laminar and obeying the Boussinesq approximation. The effects of joule heating, induced magnetic field and viscous dissipation are neglected. The base fluid and the nanoparticles are assumed to be in thermal equilibrium and their thermo-physical properties are taken from Bansal et.al. [15].

Thus, the steady governing equations of conservation of mass, momentum and energy in dimensionless form can be written as follows [1], [8], [12]:

$$\frac{\partial u}{\partial x}+\frac{\partial v}{\partial y}=0 \tag{1}$$

$$\begin{aligned} u\frac{\partial u}{\partial x}+v\frac{\partial u}{\partial y} &= -\frac{\partial p}{\partial x}+\frac{\mu_{nf}}{\rho_{nf}\alpha_f}\nabla^2 u \\ &\quad +Ha^2 Pr\sin\gamma\left(v\cos\gamma-u\sin\gamma\right) \end{aligned} \tag{2}$$

$$\begin{aligned} u\frac{\partial v}{\partial x}+v\frac{\partial v}{\partial y} &= -\frac{\partial p}{\partial y}+\frac{\mu_{nf}}{\rho_{nf}\alpha_f}\nabla^2 v+RaPr\frac{(\rho\beta)_{nf}}{\rho_{nf}\beta_f}\theta \\ &\quad +Ha^2 Pr\cos\gamma\left(u\sin\gamma-v\cos\gamma\right) \end{aligned} \tag{3}$$

$$u\frac{\partial \theta}{\partial x}+v\frac{\partial \theta}{\partial y} = \frac{\alpha_{nf}}{\alpha_f}\left(\frac{\partial^2\theta}{\partial x^2}+\frac{\partial^2\theta}{\partial y^2}\right) \tag{4}$$

by defining the dimensionless parameters as

$$\begin{aligned} &x=\frac{\bar{x}}{\ell},\ y=\frac{\bar{y}}{\ell},\ u=\frac{\bar{u}\ell}{\alpha_f},\ v=\frac{\bar{v}\ell}{\alpha_f},\ p=\frac{\bar{p}\ell^2}{\rho_{nf}\alpha_f^2},\\ &\theta=\frac{\overline{T}-T_c}{T_h-T_c},\ Ha=B_0\ell\sqrt{\frac{\sigma_{nf}}{\rho_{nf}\nu_f}},\ Pr=\frac{\nu_f}{\alpha_f},\\ &Ra=\frac{g\beta_f\ell^3(T_h-T_c)}{\nu_f\alpha_f} \end{aligned} \tag{5}$$

where the overline in equation (5) indicates the quantities are dimensional. The parameters ℓ, g, σ, ν and B_0 are the characteristic length, gravitational acceleration, electrical conductivity, kinematic viscosity and the magnetic field intensity, respectively. In equations (1)-(4) u, v, p and θ denote the dimensionless x- and y-velocity components, pressure and temperature of the fluid, respectively. Here Pr, Ra and Ha represent, respectively, Prandtl, Rayleigh and Hartmann

numbers. The thermo-physical properties of nanofluids are defined by the following formulas [15]:

$$\begin{aligned}
&\rho_{nf} = (1-\phi)\rho_f + \phi\rho_p, \quad \sigma_{nf} = (1-\phi)\sigma_f + \phi\sigma_p,\\
&(\rho\beta)_{nf} = (1-\phi)(\rho\beta)_f + \phi(\rho\beta)_p, \quad \alpha_{nf} = k_{nf}/(\rho C_p)_{nf},\\
&(\rho C_p)_{nf} = (1-\phi)(\rho C_p)_f + \phi(\rho C_p)_p, \quad \mu_{nf} = \frac{\mu_f}{(1-\phi)^{2.5}}
\end{aligned} \tag{6}$$

where ϕ is the nanoparticle volume fraction, ρ is the density, α is the thermal diffusivity, C_p is the specific heat, β is the thermal expansion coefficient, μ is the effective dynamic viscosity, k is the thermal conductivity. The subscripts '$_{nf}$', '$_f$' and '$_p$' refer to nanofluid, fluid and nanoparticle, respectively. Finally, the thermal conductivity of the nanofluid is given as

$$k_{nf} = k_f \left[\frac{k_p + 2k_f - 2\phi(k_f - k_p)}{k_p + 2k_f + \phi(k_f - k_p)} \right] .$$

The appropriate dimensionless boundary conditions corresponding to the considered problem are

$$\begin{aligned}
&\text{At left wall:} && u = 0 = v = 0,\ \theta = 1\\
&\text{At right wall:} && u = v = 0,\ \theta = 0\\
&\text{At horizontal walls:} && u = v = 0,\ \partial\theta/\partial n = 0\\
&\text{On the cylinder surface:} && u = v = 0,\ \partial\theta/\partial n = 0\,.
\end{aligned} \tag{7}$$

The system of equations (1)-(4) can be written in the stream function ψ, vorticity w and temperature form as

$$\nabla^2\psi = -w \tag{8}$$

$$\begin{aligned}
\frac{\mu_{nf}}{\rho_{nf}\alpha_f}\nabla^2 w = \frac{\partial w}{\partial x}\frac{\partial \psi}{\partial y} - \frac{\partial w}{\partial y}\frac{\partial \psi}{\partial x} - RaPr\frac{(\rho\beta)_{nf}}{\rho_{nf}\beta_f}\frac{\partial\theta}{\partial x}\\
-Ha^2Pr\left(\sin 2\gamma\frac{\partial^2\psi}{\partial x\partial y} + \cos^2\gamma\frac{\partial^2\psi}{\partial x^2} + \sin^2\gamma\frac{\partial^2\psi}{\partial y^2}\right)
\end{aligned} \tag{9}$$

$$\frac{\alpha_{nf}}{\alpha_f}\nabla^2 T = \frac{\partial T}{\partial x}\frac{\partial\psi}{\partial y} - \frac{\partial T}{\partial y}\frac{\partial\psi}{\partial x} \tag{10}$$

by defining the stream function ψ and the vorticity w as

$$\frac{\partial\psi}{\partial y} = u, \quad \frac{\partial\psi}{\partial x} = -v, \quad w = \frac{\partial v}{\partial x} - \frac{\partial u}{\partial y}\,. \tag{11}$$

The corresponding boundary conditions for stream function and temperature become

$$\begin{aligned}
&\text{At left wall:} && \psi = 0,\ \theta = 1\\
&\text{At right wall:} && \psi = 0,\ \theta = 0\\
&\text{At horizontal walls:} && \psi = 0,\ \partial\theta/\partial n = 0\\
&\text{On the cylinder surface:} && \psi = 0,\ \partial\theta/\partial n = 0
\end{aligned} \tag{12}$$

and the unknown boundary conditions for the vorticity will be obtained from equation (8) by using a radial basis function approximation which is an advantage of DRBEM.

In order to determine the heat transfer enhancement in the cavity, the local Nusselt number Nu based on the height of the cavity is evaluated by [15]

$$Nu = -\frac{k_{nf}}{k_f}\frac{\partial\theta}{\partial n}|_{wall}$$

while the surface average Nusselt number $\overline{Nu}$ is obtained by integrating its local value on the concerned surface.

III. Method of solution and numerical verification

The governing equations (8)-(10) subjected to the boundary conditions (12) are discretized using the dual reciprocity boundary element method, which aims to transform these equations into boundary only integral equations by means of a radial basis function approach. Equations (8)-(10) are weighted with the fundamental solution of Laplace equation $u^* = -1/2\pi \ln r$ by treating the terms on the right hand side of these equations as inhomogeneity [16]. Thus, after the application of divergence theorem, equations (8)-(10) take the form

$$c_i S_i + \int_\Gamma (q^* S - u^*\frac{\partial S}{\partial n})d\Gamma = -\int_\Omega b_S u^* d\Omega \tag{13}$$

where S is used for each unknown ψ, w and θ. Here, Γ is the boundary of the computational domain Ω, $q^* = \partial u^*/\partial n$ and the constant $c_i = \eta_i/2\pi$ with the internal angle η_i at the source point i. The right hand side terms in equations (8)-(10) are denoted by b_S and they are approximated by using polynomial type radial basis functions f_j linked with the particular solutions $\hat{u}_j$ to equation $\nabla^2\hat{u}_j = f_j$ [16]. That is, these approximation are given by $b_S \approx \sum_{j=1}^{N+L}\alpha_{S_j} f_j = \sum_{j=1}^{N+L}\alpha_{S_j}\nabla^2\hat{u}_j$ where α_{S_j} are undetermined coefficients, N and L are the number of boundary and interior nodes, respectively. Thus, equation (13) take the form

$$\begin{aligned}
c_i S_i + \int_\Gamma (q^* S - u^*\frac{\partial S}{\partial n})d\Gamma =\\
\sum_{j=1}^{N+L}\alpha_{S_j}\left[c_i\hat{u}_{ji} + \int_\Gamma (q^*\hat{u}_j - u^*\hat{q}_j)d\Gamma\right]
\end{aligned} \tag{14}$$

which contains only boundary integrals and $\hat{q} = \partial\hat{u}_j/\partial n$. By discretizing the boundary with constant elements, the matrix-vector form of equation (14) can be expressed in a compact way for each unknowns $S(=\psi,\ w,\ \theta)$, as

$$HS - G\frac{\partial S}{\partial n} = (H\hat{U} - G\hat{Q})F^{-1}b_S \tag{15}$$

where the matrices $\hat{U}$ and $\hat{Q}$ are constructed by taking each of the vectors $\hat{u}_j$ and $\hat{q}_j$ as columns, respectively. The matrix F consists of vectors f_j of size $(N+L)$ as columns. The components of the matrices G and H are obtained by taking the integral of the fundamental solution u^* and its normal derivative along each boundary elements Γ_j, respectively. The final DRBEM equations (15) are coupled so that they are solved iteratively. In each iteration, the required space derivatives of the unknowns ψ, w and θ, and also the unknown vorticity boundary conditions are obtained by using the coordinate matrix F [16].

The present numerical algorithm is validated against the existing numerical results of [12], [17] for a two-dimensional natural convection flow in a square cavity filled with Cu-water nanofluid. In this problem, the top and bottom walls are adiabatic while the left wall is heated and the right wall is cold. Table I shows the values of the average Nusselt number

along the hot wall of the cavity, which are computed with the present algorithm and are given in the works [12], [17], for various Grashof numbers and the solid volume fraction $\phi = 0.04, 0.2$. The values of $\overline{Nu}$ in work of Khanafer [17] are obtained from the correlation (23) in [17]. The obtained results are in good agreement with those of [12], [17].

TABLE I
COMPARISON OF AVERAGE NUSSELT NUMBER ON HOT WALL FOR THE NATURAL CONVECTION FLOW IN CU-WATER FILLED SQUARE CAVITY.

	$\phi = 0.04$		$\phi = 0.2$		
Gr	Present	Khanafer[17]	Present	[17]	Kobra[12]
10^3	2.0895	2.1182	2.7975	2.7645	2.5662
10^4	4.3542	4.3478	5.8641	5.6744	5.4050
10^5	9.1849	8.9243	12.121	11.647	10.667

IV. RESULTS AND DISCUSSION

In the present study, the numerical simulations with DRBEM are performed for various combination of problem parameters including Rayleigh number ($10^3 \leq Ra \leq 10^6$), Hartmann number ($0 \leq Ha \leq 100$) and the solid volume fraction ($0 \leq \phi \leq 0.2$) at fixed Prandtl number $Pr = 6.2$. The computational domain is determined by taking the height of the cavity $\ell = 1$ and the diameter of the circular cylinder $d = 0.2$. The boundary of the square cavity and the inner circular cylinder are discretized by using 120 and 60 ($N = 180$) constant boundary elements, respectively. The choice of this grid is based on the tests implying various grid sizes for the case when $Ra = 10^5$ and $Ha = 50$ are employed at $\phi = 0.1$, $d = 0.2$ and $\gamma = 0$. The results are displayed in Figure 2 in terms of $|\psi|_{\max}$ and the average Nusselt number $\overline{Nu}$ along the hot left wall. It is observed that the grid with $N \approx 180$ shows little difference with the results obtained for finer grids. Thus, the grid of $N = 180$ elements ensures grid independence and hence is used in the subsequent computations.

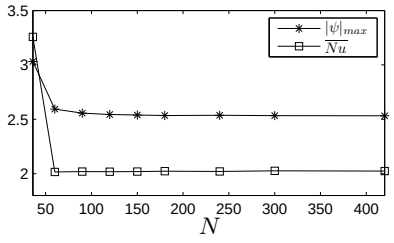

Fig. 2. Grid dependency when $Ra = 10^5$, $Ha = 50$, $\phi = 0.1$, $\gamma = 0$.

The effects of the Rayleigh number and the nanoparticle volume fraction on the flow patterns and the temperature distribution are displayed for horizontally applied magnetic field ($\gamma = 0$) when $Ha = 0$, $Ha = 30$ and $Ha = 50$ in Figures 3, 4 and 5, respectively. In these figures solid-lines and dotted-lines represent the cases with nanofluid ($\phi = 0.1$) and with pure fluid ($\phi = 0$), respectively. It is observed that in the absence of magnetic field ($Ha = 0$), adding nanoparticles leads to an increase in the magnitude of maximum stream function at $Ra = 10^4, 10^5, 10^6$, while it decreases in the conduction dominated case at $Ra = 10^3$. However, in the presence of magnetic field the strength of the stream function decreases due to the retarding effect of magnetic field on the fluid flow, therefore, addition of nanoparticles results in weaker buoyancy driven circulations, which reduces the values of stream function. By increase of the buoyant force via increasing Ra, the strength of ψ increases and the streamlines become dense close to the vertical walls of the cavity forming secondary eddies near the circular cylinder (at $Ra = 10^5, 10^6$) for each $Ha(= 0, 30, 50)$. Moreover, the core vortex in streamlines extends vertically as Ha increase and it tends to become diagonal and finally horizontal as Ra increases. On the other hand, with an increase in Ra the free convection dominates the flow and isotherms change their profiles from being vertical to almost horizontal at the center of the cavity. However, Hartmann number has an opposite influence on

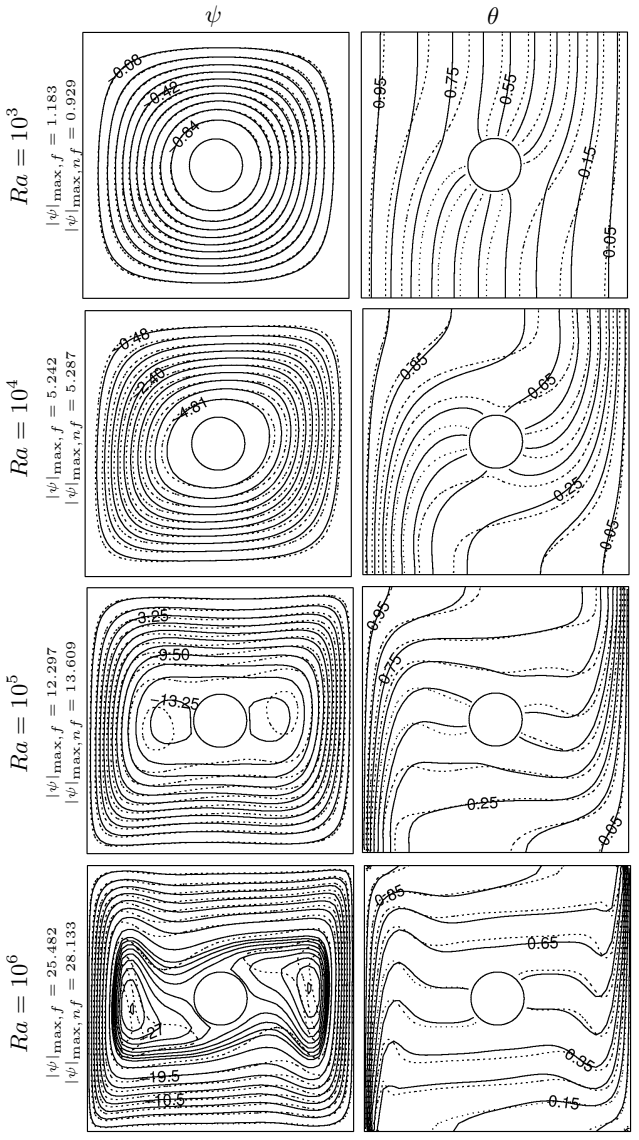

Fig. 3. Streamlines and isotherms for nanofluid with $\phi = 0.1$ (solid) and water (dotted) at different Rayleigh numbers: $Ha = 0$, $\gamma = 0$.

isotherms, that is, the isotherms tend to go from horizontal to vertical (especially at $Ra = 10^5$) indicating the suppression of convective flows at higher Ha. Moreover, following an increase in Ra, isotherms are condensed close to vertical

walls, which results in a thermal boundary layer formation along these walls at $Ra = 10^5, 10^6$ when $Ha = 0, 30$ and at $Ra = 10^6$ when $Ha = 50$. It is also observed from isotherms that at each Rayleigh number with the addition of nanoparticles the thermal boundary layer along the vertical walls becomes thicker due to higher conductivity of nanofluid than that of pure fluid. These results are compatible with the ones given in [12].

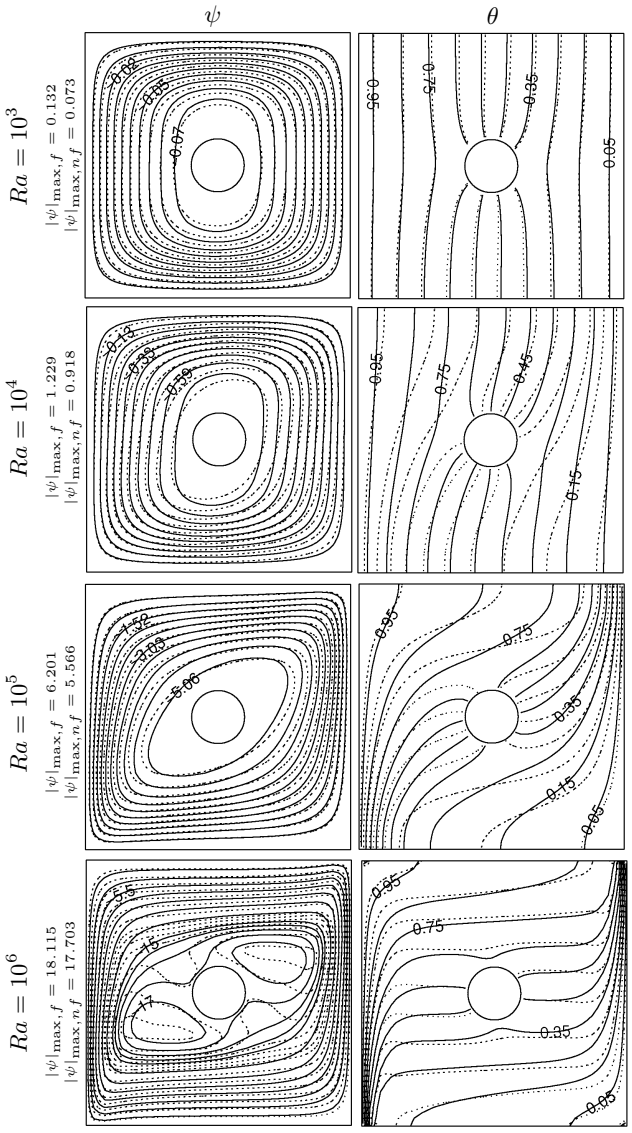

Fig. 4. Streamlines and isotherms for nanofluid with $\phi = 0.1$ (solid) and water (dotted) at different Rayleigh numbers: $Ha = 30$, $\gamma = 0$.

In Figure 6, the variation of average Nusselt number on the left hot wall with Hartmann and Rayleigh numbers are shown for the nanofluid with $\phi = 0.1$ when $\gamma = 0$. It is observed that there is no difference in $\overline{Nu}$ at different Hartmann numbers when the heat transfer is dominated by conduction at $Ra = 10^3$, indicating that Ha has no significant effect on heat transfer. However, for higher values of Ra, $\overline{Nu}$ decreases as Ha increases since the magnetic field reduces the flow and consequently the convective heat transfer is decreased. Furthermore, the rate of decrease in $\overline{Nu}$ for higher

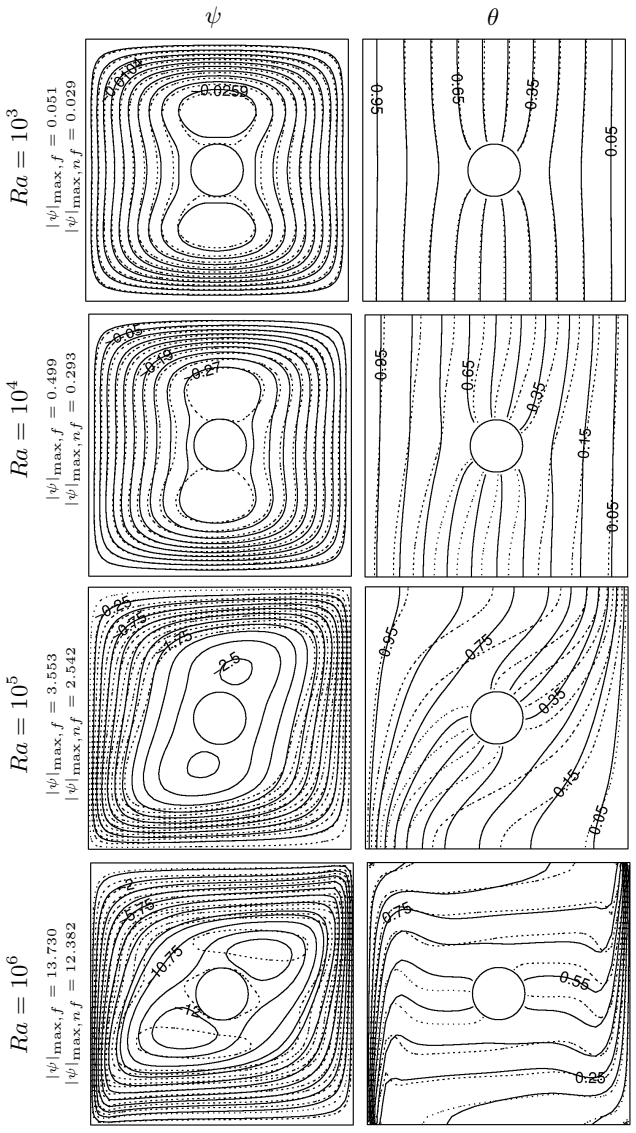

Fig. 5. Streamlines and isotherms for nanofluid with $\phi = 0.1$ (solid) and water (dotted) at different Rayleigh numbers: $Ha = 50$, $\gamma = 0$.

Ha increases with an increase in Ra. On the other hand, $\overline{Nu}$ increases as Ra increases since the heat transfer is due to convection, and the increase rate is higher in the absence of magnetic field ($Ha = 0$).

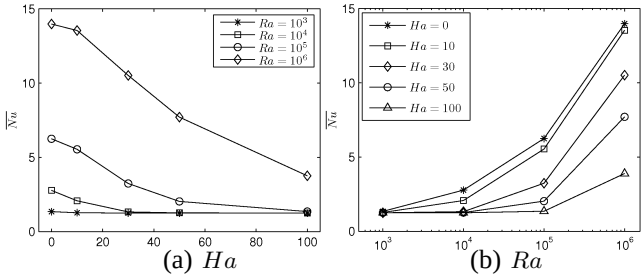

Fig. 6. Effects of (a) Hartmann number and (b) Rayleigh number on average Nusselt number at $\phi = 0.1$, $\gamma = 0$.

The effect of solid volume fraction ϕ on the average Nusselt number at different values of Rayleigh number and $\gamma = 0$ is

displayed in Figure 7 (a) $Ha = 0$, (b) $Ha = 10$, (c) $Ha = 30$, (d) $Ha = 50$. At each Ha, the average Nusselt number is an increasing function of Rayleigh number for all values of solid volume fraction since the heat transfer becomes dominated by the convection for high Ra. On the other hand, when the intensity of the magnetic field is low ($Ha < 30$) the average Nusselt number increases as ϕ increases regardless of the values of Ra, which indicates that the addition of nanoparticles enhances the heat transfer rate inside the cavity. However, the amount of increase in $\overline{Nu}$ reduces as Ha increases from $Ha = 0$ to $Ha = 10$, and specifically at $Ra = 10^4$ and $Ra = 10^5$ the solid volume fraction has no significant effect on $\overline{Nu}$ following the suppression effect of magnetic field on convective flow. On the other hand, when $Ha \geq 30$ the behavior of $\overline{Nu}$ with respect to ϕ alters drastically at $Ra \geq 10^5$. That is, when $Ha \geq 30$ and $Ra = 10^5, 10^6$ an increase in solid volume fraction results in a decrease of $\overline{Nu}$ (and as a result in the reduction of heat transfer rate inside the cavity) while it increases for lower values of Ha and Ra. This result shows that the magnetic field of specific intensity plays a significant role in the heat transfer enhancement in the enclosures filled with nanofluids of different volume fractions. It is also observed that when $Ha = 30$ the heat transfer is higher for the pure fluid ($\phi = 0$) when $Ra = 10^4$. The reason for this phenomena is that at $Ra = 10^4$ the buoyancy force is not strong enough to resist the magnetic field with strength $Ha = 30$, and hence an increase in the solid volume fraction of nanofluid reduces the heat transfer rate.

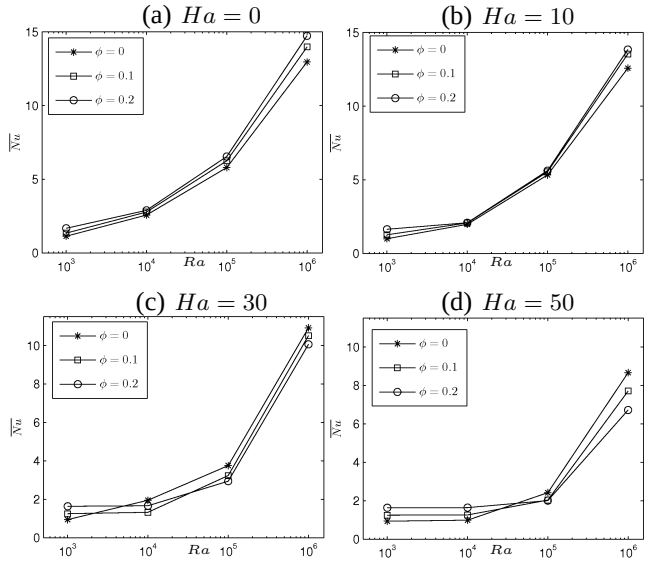

Fig. 7. Variation of average Nusselt number with Rayleigh number at different solid volume fractions $\phi(= 0, 0.1, 0.2)$ when $\gamma = 0$: (a) $Ha = 0$, (b) $Ha = 10$, (c) $Ha = 30$, (d) $Ha = 50$.

The variations of streamlines and isotherms with respect to the inclination angle of magnetic field for the nanofluid with $\phi = 0.1$ at $Ha = 30$ are visualized in Figure 8 for the conductive flow when $Ra = 10^3$ and in Figure 9 for the convective flow when $Ra = 10^5$, respectively. The average Nusselt number and the maximum magnitude of the stream function are also displayed in the figures. It is evident that

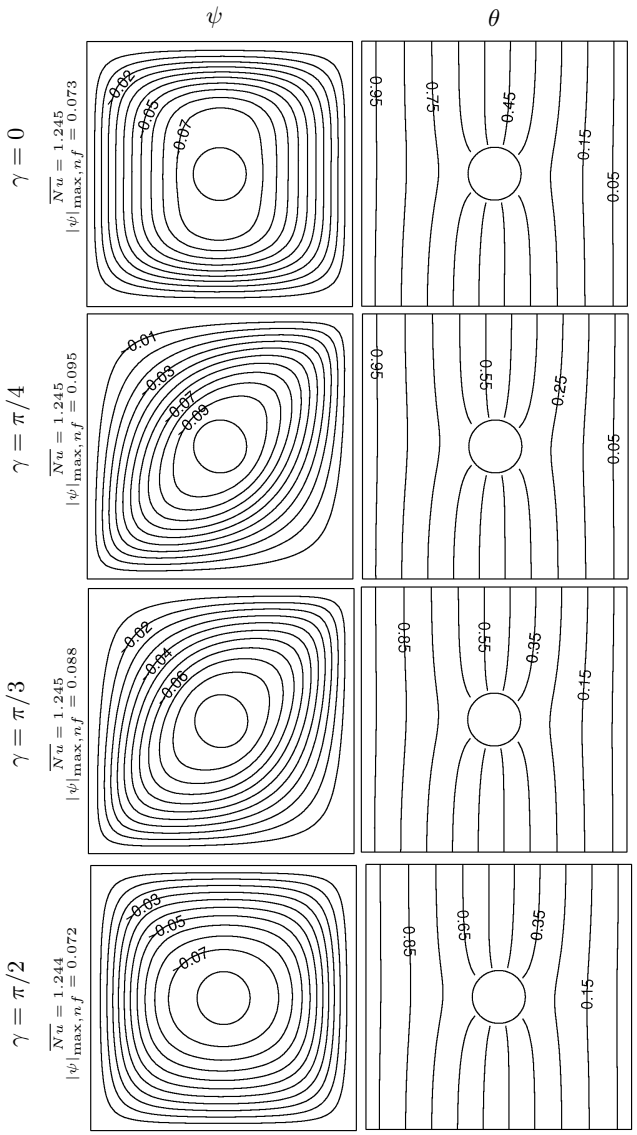

Fig. 8. Streamlines and isotherms for nanofluid with $\phi = 0.1$ at different inclination angles of magnetic field γ: $Ha = 30$, $Ra = 10^3$.

the direction of the magnetic field has a significant effect on the flow patterns. That is, the streamlines extends in the direction of magnetic field when $\gamma = \pi/4, \pi/3$ in each Ra. Furthermore, the core vortex of streamlines showing a vertical extension around the circular cylinder when $\gamma = 0$, $Ra = 10^3$ tends to extend horizontally when γ increases to $\pi/2$. A similar behavior is also seen at $Ra = 10^5$ with a small difference at $\gamma = 0$ in which the core vortex in streamlines has been almost diagonal due to the stronger convective flow at $Ra = 10^5$. The stream function increases a little in magnitude as γ increases, but then its magnitude starts to decrease with further increase in γ. On the other hand, at $Ra = 10^3$ when the heat transfer is due to mainly conduction there is no alteration in the isotherms and the values of $\overline{Nu}$ as γ increases from 0 to $\pi/2$. However at high $Ra = 10^5$ as γ increases, little variations are observed in the isotherms, especially between $\gamma = 0$ and $\gamma = \pi/2$ following the changes in $\overline{Nu}$ which is an indicator for the heat transfer rate. It seems that the

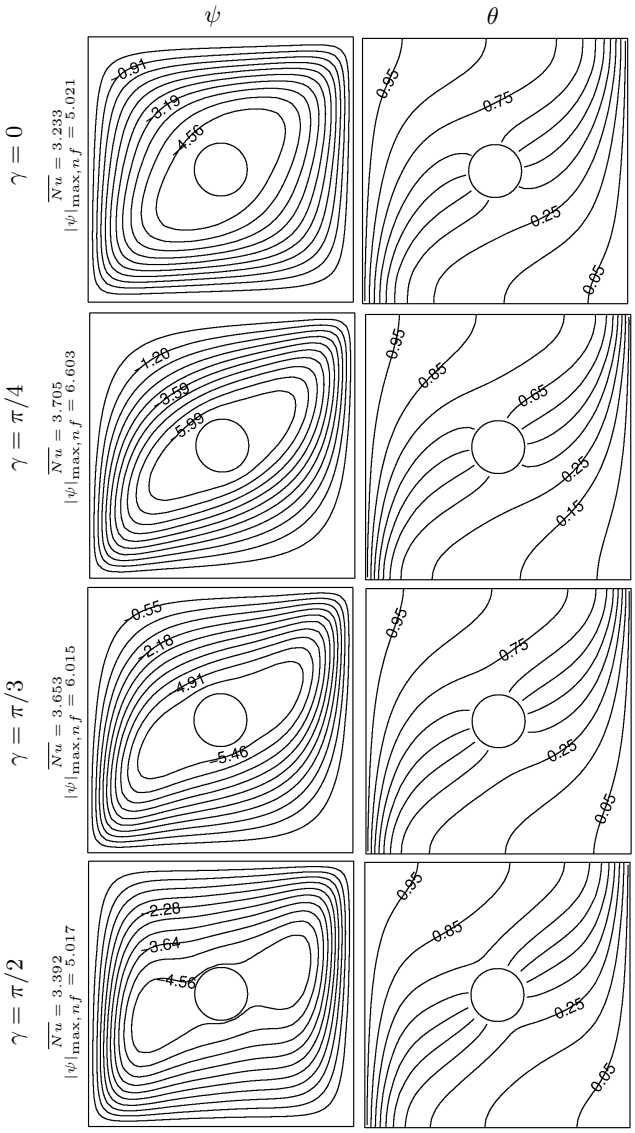

Fig. 9. Streamlines and isotherms for nanofluid with $\phi = 0.1$ at different inclination angles of magnetic field γ: $Ha = 30$, $Ra = 10^5$.

heat transfer is enhanced more at $\gamma = \pi/4, \pi/3$ compared to the cases at $\gamma = 0, \pi/2$ when the heat transfer is convection dominated at $Ra = 10^5$.

The effect of the inner circular cylinder on $\overline{Nu}$ along the hot wall of the cavity is also analyzed at various combination of Hartmann and Rayleigh numbers. The variation of $\overline{Nu}$ with respect to Ha in the presence and in the absence of the inner circular cylinder is displayed in Figure 10 at $Ra = 10^3, 10^4, 10^5$. It is observed that the average Nusselt number on the left wall increases when a circular cylinder of diameter $d = 0.2$ is inserted inside the square cavity for $Ha < 50$ when $Ra = 10^4, 10^5$. On the other hand, at the lowest Rayleigh number $Ra = 10^3$ the presence of cylinder has no effect on $\overline{Nu}$ for each Ha since the heat transfer is mainly driven by conduction. For higher values of $Ha \geq 50$ at $Ra = 10^3, 10^4$, $\overline{Nu}$ remains constant for both cases with and without cylinder and at $Ra = 10^5$ it slightly increase with the insertion of cylinder. This is a result of the suppression effect

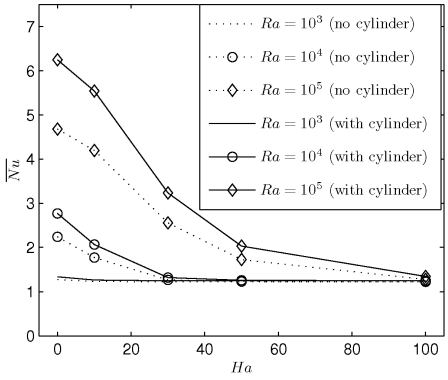

Fig. 10. Variation of average Nusselt number along the hot wall of the cavity with and without circular cylinder at $\gamma = 0$.

of the magnetic field on the convective flow, and hence on the convective heat transfer at high Ra.

V. Conclusion

The natural convection flow in a square cavity filled with Cu-water nanofluid in the presence of an inclined magnetic field is numerically solved. It is observed that the dual reciprocity boundary element method is an effective technique for the solution of MHD nanofluid natural convection in cavities with a circular cylinder, which is a rather complex problem geometry. The obtained results reveal that the flow behavior and the heat transfer enhancement are strongly influenced by the presence of magnetic field and the insertion of nanoparticles with various solid volume fractions to the fluid flow in enclosures with circular cylinder. The Hartmann and Rayleigh numbers affect the fluid flow and the heat transfer in opposite manner. That is, the flow strength and heat transfer rate increases as Rayleigh number increases, while they decreases for higher Hartmann numbers at a fixed solid volume fraction. It is further shown that the effect of suspended nanoparticles with various solid volume fractions depends strongly on the values of Hartmann and Rayleigh numbers. The nanofluid heat transfer rate increases with an increase in solid volume fraction in the case when the heat transfer is due to conduction regardless of the values of Hartmann number. However, when the heat transfer is dominated by convection via high Rayleigh numbers, the heat transfer rate decreases as solid volume fraction increases in the presence of magnetic field with high intensity. Moreover, the direction of the magnetic field vary the flow patterns significantly while the isotherms remains almost same at various inclination angles of the magnetic field.

References

[1] B. Ghasemi, S. M. Aminossadati, and A. Raisi, "Magnetic field effect on natural convection in a nanofluid-filled square enclosure," *International Journal of Thermal Sciences*, vol. 50, pp. 1748–1756, 2011.

[2] M. A. Teamah and W. M. El-Maghlany, "Augmentation of natural convective heat transfer in square cavity by utilizing nanofluids in the presence of magnetic field and uniform heat generation/absorption," *International Journal of Thermal Sciences*, vol. 58, pp. 130 – 142, 2012.

[3] H. Nemati, M. Farhadi, K. Sedighi, H. Ashorynejad, and E. Fattahi, "Magnetic field effects on natural convection flow of nanofluid in a rectangular cavity using the lattice boltzmann model," *Scientia Iranica*, vol. 19, no. 2, pp. 303 – 310, 2012.

[4] G. R. Kefayati, "Effect of a magnetic field on natural convection in a nanofluid-filled enclosure with a linearly heated wall using LBM," *Arabian Journal for Science and Engineering*, vol. 39, no. 5, pp. 4151–4163, 2014.

[5] M. Rahman, M. Alam, N. Al-Salti, and I. Eltayeb, "Hydromagnetic natural convective heat transfer flow in an isosceles triangular cavity filled with nanofluid using two-component nonhomogeneous model," *International Journal of Thermal Sciences*, vol. 107, pp. 272 – 288, 2016.

[6] M. Tezer-Sezgin, C. Bozkaya, and Önder Türk, "Natural convection flow of a nanofluid in an enclosure under an inclined uniform magnetic field," *European Journal of Computational Mechanics*, vol. 25, no. 1-2, pp. 2–23, 2016.

[7] B. Ghasemi, "Magnetohydrodynamic natural convection of nanofluids in U-shaped enclosures," *Numerical Heat Transfer, Part A: Applications*, vol. 63, no. 6, pp. 473–487, 2013.

[8] H. M. Elshehabey, F. M. Hady, S. E. Ahmed, and R. A. Mohamed, "Numerical investigation for natural convection of a nanofluid in an inclined L-shaped cavity in the presence of an inclined magnetic field," *International Communications in Heat and Mass Transfer*, vol. 57, pp. 228 – 238, 2014.

[9] N. S. Bondareva, M. A. Sheremet, and H. F. "Heatline visualization of MHD natural convection in an inclined wavy open porous cavity filled with a nanofluid with a local heater," *International Journal of Heat and Mass Transfer*, vol. 99, pp. 872 – 881, 2016.

[10] M. Sheikholeslami, D. Ganji, and M. Rashidi, "Magnetic field effect on unsteady nanofluid flow and heat transfer using Buongiorno model," *Journal of Magnetism and Magnetic Materials*, vol. 416, pp. 164 – 173, 2016.

[11] S. Aminossadati, "Hydromagnetic natural cooling of a triangular heat source in a triangular cavity with water-CuO nanofluid," *International Communications in Heat and Mass Transfer*, vol. 43, pp. 22 – 29, 2013.

[12] F. Kobra, N. Quddus, and M. A. Alim, "Heat transfer enhancement of Cu-water nanofluid filled in a square cavity with a circular disk under a magnetic field," *Procedia Engineering*, vol. 90, pp. 582 – 587, 2014, 10th International Conference on Mechanical Engineering, ICME 2013.

[13] F. Selimefendigil and H. F. "Natural convection and entropy generation of nanofluid filled cavity having different shaped obstacles under the influence of magnetic field and internal heat generation," *Journal of the Taiwan Institute of Chemical Engineers*, vol. 56, pp. 42 – 56, 2015.

[14] T. Zhang and D. Che, "Double MRT thermal lattice boltzmann simulation for MHD natural convection of nanofluids in an inclined cavity with four square heat sources," *International Journal of Heat and Mass Transfer*, vol. 94, pp. 87 – 100, 2016.

[15] S. Bansal and D. Chatterjee, "Magneto-convective transport of nanofluid in a vertical lid-driven cavity including a heat-conducting rotating circular cylinder," *Numerical Heat Transfer, Part A: Applications*, vol. 68, no. 4, pp. 411–431, 2015.

[16] C. A. Brebbia, P. W. Partridge, and L. C. Wrobel, *The Dual Reciprocity Boundary Element Method*. Southampton, Boston: Computational Mechanics Publications, 1992.

[17] K. Khanafer, K. Vafai, and M. Lightstone, "Buoyancy-driven heat transfer enhancement in a two-dimensional enclosure utilizing nanofluids," *International Journal of Heat and Mass Transfer*, vol. 46, no. 19, pp. 3639 – 3653, 2003.